Functional characterization of rose phenylacetaldehyde reductase (PAR), an enzyme involved in the biosynthesis of the scent compound 2-phenylethanol

Functional characterization of rose phenylacetaldehyde reductase (PAR), an enzyme involved in the biosynthesis of the scent compound 2-phenylethanol

Xiao-Min Chen,[1] Hiromi Kobayashi,[2] Miwa Sakai,[3] Hiroshi Hirata,[1] Tatsuo Asai,[2] Toshiyuki Ohnishi,[4] Susanne Baldermann,[1] and Naoharu Watanabe[2]*

[1]Graduate School of Science and Technology, Shizuoka University,
836 Ohya, Suruga-ku, Shizuoka 422-8529, Japan

[2]Faculty of Agriculture, Shizuoka University,
836 Ohya, Suruga-ku, Shizuoka 422-8529, Japan

[3]The United Graduate School of Agricultural Science, Gifu University,
836 Ohya, Suruga-ku, Shizuoka 422-8529, Japan

[4]Division of Global Research Leaders, Shizuoka University,
836 Ohya, Suruga-ku, Shizuoka 422-8529, Japan.

* Corresponding author. Tel/Fax: +81-54-238-4870

E-mail address: acnwata@agr.shizuoka.ac.jp (N. Watanabe)

Summary

24

25   2-Phenylethanol (2PE) is a prominent scent compound released from flowers

26 of Damask roses (*Rosa ×damascena*) and some hybrid roses (*Rosa* 'Hoh-Jun' and

27 *Rosa* 'Yves Piaget'). 2PE is biosynthesized from L-phenylalanine (L-Phe) *via* the

28 intermediate phenylacetaldehyde (PAld) by two key enzymes, aromatic amino acid

29 decarboxylase (AADC) and phenylacetaldehyde reductase (PAR).

30   Here we describe substrate specificity and cofactor preference in addition to

31 molecular characterization of rose-PAR and recombinant PAR from *R. ×damascena*.

32 The deduced amino acid sequence of the full-length cDNA encoded a protein

33 exhibiting 77% and 75% identity with *Solanum lycopersicum* PAR1 and 2,

34 respectively. The transcripts of *PAR* were higher in petals than calyxes and leaves

35 and peaking at the unfurling stage 4. Recombinant PAR and rose-PAR catalyzed

36 reduction of PAld to 2PE using NADPH as the preferred cofactor. Reductase activity

37 of rose-PAR and recombinant PAR were higher for aromatic and aliphatic aldehydes

38 than for ketocarbonyl groups. The both PARs showed that [4S-^{2}H] NADPH was

39 preferentially used over the [4R-^{2}H] isomer to give [1-^{2}H]-2PE from PAld, indicating

40 that PAR can be classified as short-chain dehydrogenase reductase (SDR).

41 **KEYWORDS**

42 Enantio-selectivity; Phenylacetaldehyde reductase; 2-Phenylethanol; *Rosa*

43 *×damascena*; Recombinant enzyme; Substrate specificity

44 **Abbreviations**

45 AADC, Aromatic amino acid decarboxylase; PAld, Phenylacetaldehyde; PAR,

46 Phenylacetaldehyde reductase; 2PE, 2-Phenylethanol; L-Phe, L-Phenylalanine.

1   **Introduction**

2   2-Phenylethanol (2PE) is a volatile compound with a pleasant fruity, floral

3 odor and is a major constituent of rose-like flowers scents. For example, 2PE

4 occupies 60% of the total volatiles in the essential oil of Damask roses (Rusanov et al.,

5 2005). Fruits, vegetables and foods such as cheese, bread, wine, and olive oil contain

6 2PE as a major flavor compound (Lee and Richard, 1984; Rodopulo et al., 1985;

7 Clark, 1990; Jollivet et al., 1992; Gassenmeier and Schieberle, 1995). Cosmetics

8 industry uses a large amount of 2PE as ingredients in perfume and other formulations

9 because of its popular rose-like smell (Clark, 1990; Fabre et al., 1998). Esters of 2PE,

10 especially phenylethyl acetate, are also valuable fragrance compounds (Bauer et al.,

11 2001). Increasing demand for natural flavors has led to a growing interest in

12 industrial-scale 2PE biosynthesis. Under US Food and Drug Administration products

13 derived from biotechnological processes can be labeled as "natural" based on US

14 Food and Drug Administration or regulations (Serra et al., 2005). 2PE also has

15 important biological functions in plants, such as antimicrobial properties (Berrah et al.,

16 1962) and reproduction *via* its attraction of pollinating insects (Pichersky and

17 Gershenzon, 2002). Therefore studies on regulation of 2PE biosynthesis and its

18 emission are very important subjects to be clarified. As a consequence, there has

19 been much interest in the biosynthesis pathway of 2PE in plants, as well as in bacteria

20 and yeast.

21   The rose 2PE biosynthetic pathway was at one time thought to convert L-

22 phenylalanine (L-Phe) *via* phenylpyruvate and phenyl acetic acid (Bugorskii and

23 Zaprometov, 1978). We demonstrated that L-Phe is a precursor of 2PE in rose

24 flowers using feeding experiments with labeled [^{2}H] L-Phe (Watanabe et al., 2002;

25 Hayashi et al., 2003). Recently, a specific enzyme PAAS (phenylacetaldehyde

26 synthase) involved in the conversion of L-Phe to phenylacetaldehyde (PAld) was

27 isolated and characterized from *Petunia hybrida* cv. Mitchell (Kaminaga et al., 2006).

28 This PAAS belongs to group II pyridoxal 5'-phosphate-depentent amino acid

29 decarboxylases (AADCs). The AADC responsible for conversion of L-Phe to PAld

30 and also the first two rose-derived phenylacetaldehyde reductases (PAR) found to

31 catalyze the conversion of PAld to 2PE, which is the final reduction step of the

32 biosynthetic pathway, have yet been characterized in *Solanum lycopersicum* (AADC1,

33 AADC2, PAR1, PAR2) (Tieman et al., 2006, 2007). The *Solanum lycopersicum*

34   PAR1 is a member of short-chain dehydrogenase/reductase family, strongly prefers

35   PAld as substrate and does not catalyze the reverse reaction however *Solanum*

36   *lycopersicum* PAR2 has similar affinities for PAld, benzaldehyde and

37   cinnamaldehyde. The contribution of AADC generating PAld from L-Phe, and PAR

38   in the biosynthesis of 2PE *via* the intermediate PAld has been confirmed in *R*. 'Hoh-

39   Jun' (Sakai et al., 2007). Recently, the function of PAAS has been confirmed by

40   application of a *Saccharomyces cerevisia aro10*Δ mutant (Farhi et al., 2010).

41   To elucidate biochemical functions and molecular biological properties of

42   rose-PAR involved in biosynthesis of 2PE, we characterized these properties. We

43   purified a rose-PAR from *Rosa ×damascena* (Mabberley, 2008) and obtained partial

44   peptide sequences based on TOF-MS analysis. We demonstrated that the full length

45   cDNA encodes a functional PAR. Enzymatic analysis showed that the rose-PAR

46   prefers PAld, but also converts several aldo- and keto-compounds. The recombinant

47   PAR and rose-PAR showed similar substrate utilizing properties, however higher

48   turnover rates were shown in the recombinant PAR with several substrates.

49   Furthermore, the classification of PAR was discussed for rose-PAR and recombinant

50   PAR based on the stereo-selectivity toward *S*-and *R*-[4-^{2}H] NADPH.

Material and methods

Plant materials

53   Damask roses (*Rosa ×damascena* Mill.) were grown at the Field Research

54   Center, Faculty of Agriculture, Shizuoka University, Japan. Flowers at stage 2

55   (Sepals haven't started to loosen, petals completely closed), stage 4 (outer whorl of

56   petals is fully open, inner whorl starts to loosen) and stage 6 (petals are fully open,

57   stamens are invisible; *ibid.*) were collected between April and May (2004-2009)

58   (Hayashi et al., 2004). Flowers at stages 2, 4, and 6 and leaves were applied for

59   transcripts expression experiments, and flowers at stage 4 were utilized for all the

60   enzyme experiments.

Partial purification of rose-PAR

62   Floral extracts were prepared as described by Sakai et al. 2007. Briefly,

63   flowers were homogenized in chilled buffer A (10 mM potassium phosphate buffer

64   (pH 8.0), 5 mM DTT, 0.05% CHAPS, and 1% glycerol, 4 °C) and after centrifugation

65 (4000 *g*, 20 min, 4 °C) the resulting crude cell extracts were applied to ECONO pack

66 Q cartridges (5 mL, Bio-Rad). Enzymatic active fractions were eluted with a linear

67 gradient of 0-1 M KCl in buffer A at a flow rate of 1.5 mL min^{-1}. Fractions with

68 enzyme activity were salted out with 150 mM KCl and equilibrated in buffer A. The

69 diluted solutions were applied to two in-line blue HP columns (1 mL, GE Healthcare)

70 equilibrated with buffer A. After washing the column with buffer A, enzymatic active

71 fractions were eluted with a gradient of 0-150 mM KCl in buffer A at a flow rate of 1

72 mL min^{-1}. The gradient was 100-120 mM KCl within 5 min, 120-150 mM KCl

73 within 3 min, and maintained for 5 min. PAR-containing fractions were used for the

74 functional analysis. For sequencing the PAR fractions were combined and

75 concentrated by centrifugal filtration (Nanosep 10 K, PALL Life Science) before

76 application (200 μL) to a Superdex 75 10/300 GL column (GE Healthcare)

77 equilibrated with buffer A. The enzyme was eluted with 5 mL 150 mM KCl at a flow

78 rate of 0.5 mL min^{-1}. The proteins were separated on the SDS-PAGE (12% acryl

79 amide) and rose-PAR was detected at 35 kDa after Coomassie Brilliant Blue staining.

80 **Molecular mass and partial amino acid sequence of PAR**

81   The partial purified PAR enzyme was further purified by SDS-PAGE. Target

82 bands detected at ca 35 kDa were excised and digested to peptides with trypsin for

83 LC/MS/MS analysis (LC: Waters Nano Acquity, MS/MS: Waters-Micromass Q-ToF

84 Premier). Five micro-liter of digest solution were injected and desalted on a trap

85 column (0.18 × 20 mm, Nano Acquity, Waters) at a flow rate of 4 μL min^{-1} with

86 solvent A (0.1% formic acid) for 3 min. The peptides were separated on a C18

87 column (75 μm × 100 mm, Nano Acquity UPLC Beh, Waters). A linear gradient was

88 developed 0-1 min: 3% solvent B (acetonitrile, 0.1% formic acid), 30 min: 40% B,

89 32-37 min: 95% B, 37 min: 95% B, 39 min: 3% B at a flow rate of 300 nL min^{-1}. The

90 column temperature was 35 °C. The Q-TOF spectrometer was operated in the data

91 dependent acquisition (DDA) mode using an ESI(+) MS survey scan on two different

92 precursor ions. The peptide masses and sequences obtained were either matched

93 automatically to proteins in the non-redundant database (NCBI) using the Mascot

94 MS/MS ions search algorithm (http:// www.matrixscience.com).

95 **Molecular cloning of *PAR* from *Rosa ×damascena* Mill.**

96   Total RNA was isolated from the flower petals of *R. ×damascena* with a

97 RNeasy Plant Mini Kit (QIAGEN). First strand cDNA was synthesized with AMV

98 Reverse Transcriptase XL and Oligo dT- Adaptor Primer (TaKaRa RNA Kit 3.0).

99 Full-length sequences of *PAR* in rose were obtained using degenerate primers

100 designed from the amino acid sequences (No.1-3, Table 1). 3'-RACE PCR reactions

101 were performed using 3'RACE-F1, 3'RACE-F2 and 3'RACE-F3 as forward primers

102 (Supplementary Table 1). Amplified cDNAs were inserted into pCR 2.1 vector

103 (Invitrogen) and transformed into DH5α competent cells (TaKaRa). Isolated cDNA

104 was sequenced using a Thermo Sequenase cycling sequencing kit (USB Corporation)

105 on a LI-COR DNA sequencer (Model 4200L, Li-COR).

106   A 5'-RACE system kit was used for amplification of 5' ends (Invitrogen).

107 The gene-specific primers (GSP) for 5'-RACE amplifications were designed based on

108 the sequences obtained by 3'-RACE reactions (Supplementary Table 1).   Reverse

109 transcription from total RNA was performed using 5'-end-phosphorylated primer

110 (GSP1) and SuperScript™ II (5' RACE System for Rapid Amplification of cDNA

111 Ends, Invitrogen). The first PCR was performed using GSP2 primer and the abridged

112 Anchor Primer (Invitrogen). Nested PCR was then performed using the GSP3 primer

113 and Abridged Universal Amplification Primer (AUAP). Finally, end-to-end PCR was

114 performed using PAR-F-1 as forward primer and PAR-R-1 as reverse primer

115 (Supplementary Table 1). Nucleotide sequences were subsequently determined as

116 described previously.

Expression and purification of recombinant PAR protein

118   *Bam*HI and *Sal*I sites were created on the 5' and 3'-ends of *PAR* by PCR using

119 the primers PAR-F-E and PAR-R-E, respectively. The engineered cDNA fragments

120 were inserted into the *Bam*HI-*Sal*I sites of pGEX-4T-1 (GE Healthcare), resulting in a

121 recombinant gene product with an *N*-terminal glutathione *S*-transferase (GST) protein

122 tag. Freshly transformed BL21 cells harboring pGEX-PAR or an empty pGEX vector

123 were grown at 37 °C in 50 mL LB broth with 25 μg mL^{-1} ampicillin to an O.D.$_{600}$ =

124 0.6. 2.5 mL of the liquid culture were transferred to 250 mL LB broth containing the

125 appropriate antibiotics and grown until O.D.$_{600}$ = 0.8 at 37 °C. 250 μL of 1 mM ITPG

126 solution were then added to induce production of the recombinant protein and the

127 cultures grown another 8 h at 37 °C until an O.D.$_{600}$ = 1.8. The cells were harvested

128 by centrifugation (8000 g, 10 min, 4 °C) and after addition of 12.5 mL PBS (140 mM

129 NaCl, 2.7 mM KCl, 10 mM Na_2HPO_4 and 1.8 mM KH_2PO_4 (pH 7.3)) the samples

130 were frozen at -80 °C. All protein purification steps were carried out at 4 °C. The

131 cells suspended in PBS were disrupted for 10 s 5 times by ultrasonication (UD201,

132 TOMY). After the addition of 1% Triton X-100, the samples were centrifuged at

133 7700 g for 10 min to remove cell debris. Recombinant proteins were purified from

134 the supernatant on GSTrap FF columns (5mL, GE Healthcare). GST tags were

135 removed by on-column thrombin digestion (100 units, 2 h, room temperature) (GE

136 Healthcare) and the enzyme was eluted with PBS. Thrombin was removed on a

137 HiTrap Benzamidine FF column (GE Healthcare). The purity of the recombinant

138 protein was analyzed by SDS-PAGE (12% acryl amide) as described previously

139 (Fleischmann et al., 2003). A single protein was detected at 35 kDa after Coomassie

140 Brilliant Blue staining (Supplementary Fig. 3). The recombinant PAR encoding the

141 endogenous rose-PAR was subjected to functional analysis.

142 Determination of changes in transcripts of *PAR* in *Rosa ×damascena* Mill.

143 Total RNA was extracted using Fruit-mate (TaKaRa) and purified with

144 Fastpure RNA kit (TaKaRa) followed by DNase treatment (Fermentas) to remove any

145 contaminating DNA. First-strand cDNA was synthesized from 50 ng of total RNA by

146 PrimeScript RT reagent Kit, Perfect Real Time (TaKaRa). Rose-*PAR* mRNA levels

147 in petals, calyxes, and leaves were measured by real time quantitative RT-PCR. The

148 real time RT-PCR reactions were performed utilizing the SYBR-Green I dye (SYBR

149 Premix Ex Taq, Perfect Real Time, TaKaRa). The quantification was achieved from

150 dose-response curves using β-tubline as an internal control in triplicate. Primers for

151 real time RT-PCR (PAR-Q and TUB-Q) were described in Supplementary Table 1.

152 Aldehyde and ketone selectivity

153 Activities of rose-PAR and recombinant PAR were assayed at 30 °C by

154 measuring the decrease in absorbance of NADPH at 340 nm (ε_{340}= 6.2 mM^{-1} cm^{-1},

155 Ultrospec 3000, Pharmacia Biotech) (Larroy et al., 2002). The reaction mixture (200

156 μL) (100 mM potassium phosphate (pH 7.0), recombinant enzyme (6.8 μg) /rose-

157 PAR (8.0 μg), 10 mM PAld, and 2.5 mM NADPH) was incubated at 30 °C for 10 min.

158 The reaction was quenched by the addition of 300 μL acetonitrile and centrifuged at

159   3000 g for 5 min. The relative activities of rose-PAR and recombinant PAR with

160   selected substrates (Table 2) were determined by measuring the decrease in

161   absorbance of NADPH at 340 nm using 10 mM of each substrate. Reaction

162   conditions were the same as described for the PAR assay. One unit of enzyme

163   activity was defined as the oxidation of 1 μmol NADPH min^{-1} at 30 °C. Specific

164   activity was expressed as units /mg protein which was 10.1 mU mg^{-1} for rose-PAR

165   and 0.7 mU mg $^{-1}$ for recombinant PAR.

Synthesis of S-[4-^{2}H] NADPH and R-[4-^{2}H] NADPH

167   S-[4-^{2}H] NADPH was synthesized from NADP$^+$ (0.019 mM) and [1-^{2}H]

168   glucose (0.08 mM) with 8 units of glucose dehydrogenase (*Bacillus* sp., Wako Pure

169   Chemical) in 2 mL buffer (100 mM potassium phosphate and 0.1 mM EDTA, pH 8.0)

170   at 37 °C for 1 h, and then maintained at 60 °C for 10 min (McCracken et al., 2004).

171   Deuterated NADPH was isolated by HPLC with 1 mL min^{-1} flow rate at room

172   temperature in gradient mode from 0%-100% B within 30 min using 25 mM

173   phosphorous potassium buffer (pH 7.0) and 25 mM phosphorous potassium buffer

174   (pH 7.0) and 0.5 M NH$_4$HCO$_3$ as the mobile phases (McCracken et al., 2004). S-[4-

175   ^{2}H] NADPH was obtained by a column chromatography on negative ion exchange

176   resin (HiTrap Q FF, GE Healthcare), and the concentration was determined based on

177   the absorbance at 260 nm.

178   R-[4-^{2}H] NADPH was synthesized using the stereo-specificity of alcohol

179   dehydrogenases (McCracken et al., 2004). NADP$^+$ (0.022 mM) and [^{2}H$_8$] isopropanol

180   (0.6 mM) were added to 7 mL of 25 mM Tris-HCl buffer (pH 9.0). The reaction was

181   catalyzed by 8 units of alcohol dehydrogenase (*Thermoanaerobium brockii*, Sigma) at

182   43 °C for 1h and then maintained at 60 °C for 10 min. Labeled NADPH products

183   were separated by HPLC and lyophilized as above.

184   The structures and stereochemistry of S-[4-^{2}H] NADPH and R-[4-^{2}H]

185   NADPH were confirmed by one-dimensional ^{1}H-NMR spectroscopy (JNM-EX,

186   270 Hz, JEOL). The ^{1}H-NMR spectrum of non-labeled NADPH showed signals at

187   δ 2.70 (dt, J=1.8, 18.9 Hz) for 4- *pro-R* hydrogen, and at δ 2.58 (dd, J=2.7, 18.9

188   Hz) for 4-*pro-S* hydrogen. S-[4-^{2}H] NADPH showed a signal at δ 2.65 (t, J=1.8

189   Hz) for H-4, whereas a signal at δ 2.57 (d, J=2.7 Hz) was detected for 4-H of R-[4-

190   ^{2}H] NADPH. These signals were in good accordance previously published data

191 (Mostad and Glasfeld, 1993). The ratios of S-and R-[4-^{2}H] NADPH were calculated

192 to be 83% and 85% based on the intensities of proton signals assigned to 4-pro R and

193 4-pro S, respectively.

Classification of rose-PAR and recombinant PAR by elucidating the

enantio-selectivity toward R-[4-^{2}H]-NADPH or S-[4-^{2}H]-NADPH

196   To clarify the enantio-selectivity of both PARs, rose-PAR (46.8 μg) and

197 recombinant PAR (53.4 μg) were used to catalyze the reaction of 40 μL 2.5 mM PAld

198 in the presence of either R-[4-^{2}H]-NADPH or S-[4-^{2}H]-NADPH in 100 μL 100 mM

199 potassium phosphate at 30 °C for 20 min or at 60 °C for 5 min, respectively. Ethyl

200 decanoate (4 μl of 7.8 mM solution) was added as internal standard. The reaction

201 solution was extracted 3 times with a mixture of 200 μL hexane-ethyl acetate (1:1

202 v/v). The combined organic layers were dried over sodium sulfate and subjected 1 μL

203 to GC-MS analysis.

204   The GC-MS analysis was conducted on a GCMS-QP5000 (Shimadzu)

205 equipped with a SUPELCOWAX 10 column (30 mm × 0.25 mm × 0.25 μm). The

206 injector temperature was 230 °C and the samples were injected in split-less injection

207 mode. The oven temperature was set to 60°C and maintained for 3 min, and the

208 temperature increased to 180 °C at a heating rate of 40 °C min^{-1}. Finally, the

209 temperature was increased to 240 °C at a heating rate of 10 °C min^{-1} and the

210 temperature hold for 3 min. Masses were recorded from m/z 76 to 400 with an

211 electric potential of 1.25 kV. Identification of PAld and 2PE was based on a

212 comparison of their MS spectra and retention times with those of authentic samples.

213 Enantio-selectivities for chiral NADPHs were determined based on peak intensities at

214 m/z 122 [M$^+$] for 2PE and m/z 123 [M$^+$] for [1-^{2}H]-2PE.

Enantio-selectivity of the recombinant PAR toward acetophenone

216   To clarify an enantio-selectivity of recombinant PAR on the keto-carbonyl

217 moieties, acetophenone was used as a model keto-carbonyl compound. The reaction

218 of 10 mM acetophenone with 2.5 mM NADPH was catalyzed by recombinant PAR

219 (53.4 μg) in 0.1 M potassium phosphate buffer at 30 °C for 60 min, and at 60 °C for

220 10 min, respectively. Reaction products were extracted as described above and

221 subjected to GC-MS analysis. The GCMS-QP5000 (Shimadzu) was equipped with a

222   chiral InterCap CHIRAMIX column (30 mm × 0.25 mm × 0.25 μm), the oven

223   temperature was set to 40 °C for 5 min, and then temperature was increased to 180 °C

224   at a rate of 3 °C min^{-1}. Mass scan range was from *m/z* 70 to *m/z* 400 with an

225   electronic potential of 1.25 kV. The volume of injection was 1 μL. The

226   stereochemistry of 1-phenylethanol (1PE) was confirmed by authentic standards. The

227   retention times of *S*-1PE and *R*-1PE were 36.0 and 36.3 min, respectively. Enantio-

228   selectivity was determined based on the ratio of *S-/R*-1PE.

229   Results

230   Isolation of a full length rose-PAR cDNA from *Rosa ×damascena*

231   To identify the full length cDNA based on partial amino acid sequences from

232   rose-PAR, we partially purified the enzyme from petals of *R. ×damascena*.

233   Predominant PAR activities were found in fractions 21 to 23 Fig. 1A. Although

234   fraction 22 was not perfectly purified, this fraction showed the highest rose PAR

235   activity. We excised proteins of fraction 22 from the SDS-PAGE gel, especially

236   focused on the band detected at *ca* 35 kDa, based on the molecular masses of

237   *Solanum lycopersicum* PAR1 and PAR2 previously reported (Tieman et al., 2007).

238   The proteins were digested with trypsin prior to LC-MS/MS analysis of partial amino

239   acid sequences of rose-PAR.

240   *De novo* sequence analyses of the protein band (designated as band 1 in Fig.

241   1B) resulted in 11 partial peptide sequences (106 amino acids). Three degenerate

242   primers were designed for cDNA cloning based on the *de novo* sequences (Table 1).

243   As a result of 3'-RACE amplification, sequence fragments of 465 bp were determined.

244   A full-length cDNA was subsequently obtained using gene-specific primers (GSP) for

245   5'-RACE. The nucleotide sequence of this cDNA has an open reading frame of 966

246   bp that encodes a predicted protein of 322 amino acids comprising the 11 partial

247   amino acid sequences derived from the partial purified protein of rose petals

248   (Supplementary Fig. 1). Only one *PAR* cDNA was obtained from *R. ×damascena*.

249   The nucleotide sequence designated as *recombinant PAR* is available from the

250   DDBJ/EMBL databases under the accession number AB426519. The deduced amino

251   acid sequence of recombinant PAR has 77% and 75% identity with *Solanum*

252   *lycopersicum* PAR1 and PAR2, respectively. Phylogenetic analysis of the deduced

253   protein sequence showed high similarity with aldehyde reductases, such as cinnamyl

254 alcohol dehydrogenases and cinnamyl CoA reductases from many plant species

255 (Supplementary Fig. 2). The protein encoded by *PAR* cDNAs was closely related to a

256 putative cinnamyl alcohol dehydrogenase from *Malus domestica* (90% identity) and

257 *Prunus mume* (89% identity) (Mita et al., 2006). The recombinant PAR was also

258 highly similar to two aldehyde reductases from *Solanum lycopersicum* (Tieman et al.,

259 2007) (77% identity with *PAR1* and 75% identity with *PAR2*). The recombinant PAR

260 has a calculated molecular mass of 35.4 kDa, which is in accordance with SDS-PAGE

261 results of purified recombinant and rose-PAR enzymes (Fig. 1).

Functional characterization of rose-PAR and recombinant PAR

263 To confirm that the cloned cDNA encodes a functional enzyme, reaction

264 products in the presence of NADPH and either rose-PAR or recombinant PAR were

265 analyzed by GC-MS (Supplementary Scheme 1). No reaction products were detected

266 in the absence of either PAR enzyme, whereas 2PE was detected as the sole product

267 from PAld in the presence of either rose-PAR or recombinant PAR, indicating that

268 both proteins exhibit the same functions (Fig. 2).

Changes in transcripts of rose-*PAR*

270 To further substantiate rose-*PAR's* involvement in the biosynthesis of 2PE,

271 expression of rose-*PAR* transcripts in petals, calyxes at stages 2, 4, and 6, and leaves

272 were investigated by real time RT-PCR (Fig. 3). In *R. ×damascena* the transcripts of

273 rose-*PAR* were higher in petals than in calyxes and leaves. In the petals the

274 transcripts of rose-*PAR* were peaking at stage 4. There was no obvious difference in

275 the expression level of rose-*PAR* among calyxes throughout the unfurling process.

Coenzyme specificity and catalytic activity of recombinant PAR and rose-PAR

278 Recombinant PAR efficiently converted PAld to 2PE in the presence of

279 NADPH, whereas only a trace amount of 2PE was synthesized in the presence of

280 NADH (Fig. 4A). Similar results were obtained with rose-PAR. Thus, PAR is a

281 NADPH-preferring reductase.

282 Furthermore, the biosynthetic pathway proposed by Sakai et al. (2007) for

283 production of 2PE from PAld was catalyzed by PAR but the inverse reaction would

284 be hypothetically catalyzed by an alcohol dehydrogenase (ADH). The recombinant

285 PAR enzyme has around 10 times higher reductase activity than ADH activity. The

286 rose-PAR has high reductase activity with only residual ADH activity, indicating that

287 both recombinant PAR and rose-PAR predominantly catalyze the conversion of PAld

288 to 2PE (Fig. 4B).

Substrate specificity of recombinant PAR and rose-PAR

290   To understand the function of an enzyme in its metabolic pathway, enzymes

291 and their substrates must be characterized (Fridman et al., 2005). To elucidate the

292 substrate specificity of recombinant PAR and rose-PAR more in detail, 11 different

293 substrates with either aldehyde or keto moieties were tested (Table 2). Catalytic

294 efficiency of the recombinant PAR with (*S*)-(-)-citronellal was the highest among all

295 of the selected substrates, including a 3-fold increase over PAld. Hexylaldehyde also

296 had a higher turn over rate (1.9 fold) compared to PAld. Even though, the specific

297 activity of the rose-PAR (10.1 mU mg^{-1}) was much higher (10-fold) than the

298 recombinant PAR (0.7 mU mg^{-1}), both PAR enzymes showed activity with all of the

299 selected volatile compounds. The catalytic efficiencies of the rose-PAR and the

300 recombinant PAR were high using PAld, (*S*)-(-)-citronellal and hexylaldehyde as

301 substrates. These enzymes showed moderate catalytic activities with the aldehydes:

302 (*R*)-(-)-citronellal (96.9, 46.6), 3-phenylpropionaldehyde (63.6, 59.2), benzaldehyde

303 (47.3, 54.0), *trans*-cinnamaldehyde (40.3, 14.8), 2-phenylpropionaldehyde (39.5,

304 19.5), and citral (39.5, 53.9). Low activities were observed for the transformations of

305 acetophenone (28.7, 7.0) and methyl butylketone (19.0, 7.5). It can thus be inferred

306 that the catalytic efficiency of PAR is higher with aldehydes than with compounds of

307 the ketocarbonyl group. The catalytic activity of the recombinant PAR was 3-fold

308 higher with (*S*)-citronellal (311.2) than with its (*R*)-isomer (96.9) and the activity of

309 the rose-PAR was 2 times higher with (*S*)-citronellal (78.4) than with its (*R*)-isomer

310 (46.6).

Enantio-selective reduction of recombinant PAR

312   In our assay, both isomers of NADPH were labeled with mono-deuterium.

313 Incubation of the recombinant PAR and the rose-PAR with *R*-[4-^{2}H] NADPH or *S*-[4-

314 ^{2}H] NADPH resulted in 96.6% and 72.6% of [^{2}H]-2PE respectively, whereas in the

315 presence of R-[4-^{2}H] NADPH, the [^{2}H]-2PE production was lower (12.0% with the

316 recombinant PAR and 17.9% with the rose-PAR) (Fig. 5). Thus, almost 90% of the

317 PAld was converted to [^{2}H]-2PE when S-[4-^{2}H] NADPH was used. Even in the case

318 of the rose-PAR, the deuterium incorporation of S-[4-^{2}H] NADPH was 83%. Hence,

319 both PAR enzymes preferred S-[4-^{2}H] NADPH over R-[4-^{2}H] NADPH. Furthermore,

320 the reduction of PAld with S-[4-^{2}H] NADPH and the recombinant PAR was more

321 efficient (96.6% production of [^{2}H]-2PE) than with the rose-PAR (72.6% production

322 of [^{2}H]-2PE).

Stereo-selectivity of recombinant PAR

324 To investigate the stereo-selectivity of the recombinant PAR for the keto-

325 carbonyl group to yield to its corresponding secondary alcohol, acetophenone was

326 employed as model substrate (Fig. 6). Reaction mixture of acetophenone and

327 recombinant PAR yielded S-1PE in the presence of NADPH. Due to the low catalytic

328 activity of the rose-PAR with the substrate acetophenone the enantio-selectivity could

329 not be determination.

Discussion

331 We have isolated a full-length PAR cDNA from $R.$ ×$damascena$, and have

332 functionally characterized both recombinant PAR and rose-PAR. Even though a

333 protein-protein BLAST (blastp) search revealed that the obtained PAR is more similar

334 to the cinnamyl alcohol dehydrogenase from *Malus domestica* (90% identity) than to

335 the phenyl acetaldehyde reductases from *Solanum lycopersicum* (77% and 75%

336 identity), functional characterization clearly demonstrated that the PARs catalyzes the

337 transformation of PAld to 2PE. Frequently, functional enzyme annotations based on

338 sequence similarities prove to be incorrect (Fridman et al., 2005). For example, many

339 *Arabidopsis* genes annotated as putative cinnamyl alcohol dehydrogenases actually

340 encode enzymes with highly variable substrate specificities (Kim et al., 2004).

341 The GC-MS-validated functional analysis of both rose-PAR and recombinant

342 PAR confirmed that the PARs catalyze the conversion of PAld to 2PE. This study

343 revealed for the first time that rose-PAR can contribute to the production of important

344 scent molecules on molecular level. Furthermore, we investigated changes in

345 transcripts of rose-*PAR* by real time RT-PCR. Rose-*PAR* transcripts were higher in

346 petals than in calyxes and leaves. The highest transcripts have been observed at stage

347 4, suggesting a correlation to the maximum emission of 2PE at stage 4 of *R.*

348 ×*damascena* as already reported (Oka et al., 1999). Other rose scent-related genes

349 exhibited the highest transcripts at the same unfurling stage, where the emission of

350 volatile compounds was the highest (Guterman et al., 2002; Lavid et al., 2002; Farhi

351 et al., 2010). Both rose-PAR and recombinant PAR preferred NADPH over NADH

352 as coenzyme (Fig. 4A), which differs from what was observed for the PAR isolated

353 from *R.* 'Hoh- Jun' (Sakai et al., 2007). Sakai et al. had reported that both NADPH

354 and NADH could serve as cofactors for rose-PAR. Although further research is

355 needed, this discrepancy might be due to the incomplete purity of rose-PARs in the *R.*

356 'Hoh-Jun' assays. For example, in this study the PAR enzyme was separated from

357 other proteins with a 30% to 70% ammonium sulfate cut, but previously with 20% to

358 50% (Sakai et al., 2007). In this case, an enzyme could have been co-precipitated

359 with PAR which is eliminated by the higher salt concentration in the first cut.

360 Alternatively, rose cultivars may produce similar enzymes with differing substrate

361 and co-enzyme binding affinities. This would, in fact, be expected since different

362 cultivars produce different scents. For example, glucose-6-phosphate dehydrogenases

363 (G6PDHs) catalyzed the oxidation of glucose-6-phosphate to 6-phosphogluonolactone

364 concomitant with reducing NADP to NADPH, and an elevated level of cytosolic

365 glucose-6-phosphate dehydrogenases (G6PDHs) was not a consequence of phosphate

366 sequestration, but rather dependent on the presence of metabolizable sugars

367 (Hauschild and Schaewen; 2003). Furthermore, both PARs preferably catalyzed the

368 reaction from PAld to 2PE (Fig. 4B), indicating that the genuine *PAR* had been cloned

369 into *E. coli*. Consistent with our results, most cinnamyl alcohol

370 dehydrogenase/reductase enzymes, including PAR1 and PAR2 from *Solanum*

371 *lycopersicum*, also prefer NADPH as co-substrate (Tieman et al., 2007).

372   The recombinant PAR had a substrate-utilization profile similar to the rose-

373 PAR (Table 2). Both PARs favored aldehyde substrates over compounds with keto-

374 carbonyl moieties. Moreover, both PARs had higher catalytic activities on the (*S*)-

375 citronellal enantiomer, indicating that PAR activities are affected by chirality at the C-

376 6 position. The rose-PAR and the recombinant PAR differed somewhat in substrate

377 affinity. For instance, (*S*)-(-)-citronellal was the best substrate among a variety of

378 volatile compounds for the recombinant PAR, but for the native rose-PAR, PAld was

379 the best substrate. For the PAR two sugar modification motifs, NTSA in No. 201-204

380 and NASF in No. 279-282 were predicted based on the Motif search by GENETYX

381 as shown in Supplementary Fig. 1. It is generally known that proteins obtained by *E.*

382 *coli* lack in post-translational modifications. Although the sugar analysis was not

383 performed against rose-PAR, the lack in the sugar motives in recombinant PAR

384 probably is one of the reasons for the differences in the substrate specificity. It has

385 been already reported that sugar modification could affect relative enzyme functions

386 (Hauschild and Schaewen, 2003). In addition, using surfactants or CA kit (TaKaRa

387 Co. Ltd. Japan) could not overcome the different catalytic activities of rose-PAR and

388 recombinant PAR enzymes (data not shown).

389   Our group previously detected various volatile scent compounds emitted from

390 *R. ×damascena* throughout the unfurling process (Oka et al., 1999). Several

391 reductases as well as the rose-PAR may be involved in the emission of other alcoholic

392 volatile compounds such as (*S*)-(-)-citronellol and geraniol. It might be reasonable to

393 elucidate if rose-PAR plays an essential part for the production of several main rose

394 scents (Table 2). The enantio-selectivity toward *S*-[4-^{2}H] NADPH gives the basic

395 aspects on the biosynthesis of 2PE and other primary alcoholic plant volatiles from

396 the corresponding aldehydes. It may also explain the selectivity of PAR between two

397 chiral aldehydes such as (*S*)- and (*R*)-citronellal. Further research will afford the

398 evidence to explain the direction of approach for *S*-[4-^{2}H] NADPH and the substrate

399 in the active domain of the enzyme.

400   The rose-PAR and recombinant PAR exhibited moderate activities toward

401 keto-carobonyl compounds, and the latter yielded *S*-1PE from acetophenone (Table 2,

402 Fig. 6). These results may be illustrating to find the high enantio-selectivity for

403 production of chiral secondary alcohols by modifying the recombinant PAR.   Also *S*-

404 selectivity of rose-PAR toward acetophononone must be important to elucidate the role

405 in the keto-reduction in rose flowers. As neither acetophenone nor 1PE were detected

406 as volatile compounds emitted from *R. ×damascena*, this rose may not have the

407 biosynthetic systems of acetophenone. As one of the precursors of damascenone, an

408 important volatile compound found in the essential oil, we have reported (Suzuki et

409 al., 2002) the identification of glycosidic (3*R*, 9*R*)- and (3*R*, 9*S*)-megastigm-6, 7-dien

410 3, 5, 9- triol in the flowers of *R. ×damascena*. In the case of the production of these

411 compounds, a progenitor of the aglycon parts must be derived from (3*R*)-megastigm-6,

412 7-dien-9-one-3, 5-diol by the action of 9-keto-reductase. As the ratio at the 9-position

413   of glycosidic (3*R*, 9*R*)- and (3*R*, 9*S*)-megastigm-6, 7-dien 3, 5, 9- triol was 4-10 /1 for

414   *R/S*, rose-PAR is not involved in the reduction of the 9-keto-carbonyl group.

415   Furthermore, the substrate specificities and relative activities of rose-PARs

416   from *R.* ×*damascena* and *R.* 'Hoh-Jun' are generally similar (Sakai et al., 2007). For

417   instance, both native PARs had higher activities with aldehydes than with substrates

418   with ketocarbonyl moieties, and PAld was the best substrate for both native PARs.

419   However, *R.* ×*damascena* rose-PAR catalyzes reactions with a wider range of

420   substrates than *R.* 'Hoh-Jun' rose-PAR, which did not show any activity with

421   benzaldehyde, *trans*-cinnamaldehyde, acetophenone or methyl butylketone.

422   A commonly used sequence-based classification of alcohol dehydrogenases

423   defines three super-families which are differentiated, amongst other features, by the

424   molecular size of the protein chain: short-chain dehydrogenase/reductases (SDR;

425   ~250 amino acids) (Jornvall et al., 1995), medium-chain dehydrogenase/reductases

426   (MDR; ~350 amino acids per subunit) (Persson et al., 1994), and long-chain

427   dehydrogenases (LDR; ~360-550 amino acids) (Persson et al., 1991). An increasing

428   number of oxidoreductases not related to any of these superfamilies have been

429   identified as members of the aldo-keto reductase (AKR) superfamily (Bohren et al.,

430   1989). Only the AKRs are monomeric proteins among these four superfamilies, and

431   are about 320 amino acid residues in size.

432   The SDRs and LDRs utilize *pro-S* hydrogen of NADPH, whereas the MDRs

433   and AKRs utilize *pro-R* hydrogen (Costanzo et al., 2009). Thus, as a potential

434   discriminator for classification, the purified enzyme preparations were assayed with

435   *S*-, and *R*-[4-^{2}H]-NADPH to convert PAld or acetophenone. Both recombinant PAR

436   and rose-PAR preferred *S*-[4-^{2}H] NADPH over *R*-[4-^{2}H] NADPH (Fig. 5), suggesting

437   that both PARs are SDRs or LDRs rather than MDRs and AKRs. Structurally, SDR

438   functional sites contain a YXX(S)K motif, whereas the AKR cofactor-binding pocket

439   has four strictly-conserved residues (D50, Y55, K84 and H117). PAR contains a

440   YVLSK sequence at residues 60 to 64, and no AKR cofactor-binding pocket motif

441   (Supplementary Fig. 1). This suggests that recombinant PAR and rose-PAR may be

442   placed in the SDR protein super-family.

443

444   **Acknowledgements**

446 **References**

447 Albertazzi E, Cardillo R, Servi S, Zucchi G. Biogeneration of 2-phenylethanol and 2-
448   phenylethylacetatae important aroma components. Biotechnol Lett 1994;16:491-6.
449 Bauer K, Garbe D, Surburg H. Common fragrance and flavor materials preparations, prosperities and
450   uses. Weinheim: Wiley-VCH, 2001.
451 Berrah G, Konezka WA. Selective and reversible inhibition of the synthesis of bacterial
452 deoxyribonucleic acid by phenethyl alcohol. J Bacteriol 1962;83:738-44.
453 Bohren KM, Bullock B, Wermuth B, Gabbay KH. The aldo-keto reductase superfamily. J Biol Chem
454   1989;264:9547-51.
455 Bugorskii PS, Zaprometov MN. Biosynthesis of beta-phenylethanol in rose petals. Biokhimiia
456   1978;43:2038-42.
457 Clark GS. Phenylethyl alcohol. Perfum Flavor 1990;15:37-44.
458 Costanzo LD, Penning TM, Chritianson DW. Aldo-keto reductases in which the conserved catalytic
459   histidine is substituted. Chem-Biol Inter 2009;178:127-33.
460 Edman P. Method for determination of the amino acid sequence in peptides. Acta Chem Scand
461   1950;4:283-93.
462 Fabre CE, Blanc PJ, Goma G. 2-Phenylethyl alcohol: An aroma profile. Perfum Flavor 1998;23:43-5.
463 Farhi M, Lavie O, Masci T, Hendel-Rahmanim K, Weiss D, Abeliovich H, Vainstein A. Identification
464   of rose phenylacetaldehyde synthase by functional complementation in yeast. Plant Mol Biol
465   2010;72:235-45.
466 Fleischmann P, Watanabe N, Winterhalter P. Enzymatic carotenoid cleavage in star fruit (*Averrhoa*
467   *carambola*). Phytochemistry 2003;63:131-7.
468 Fridman E, Pichersky E. Metabolomics, genomics, proteomics, and the identification of enzymes and
469   their substrates and products. Curr Opin Plant Biol 2005;8:242-8.
470 Guterman I, Shalit M, Menda N, Piestun D, Dafny-Yelin M, Shalev G, Bar E, Davydov O, Ovadis M,
471   Emanuel M, Wang J, Adam Z, Pichersky E, Lewinsohn E, Zamir D, Vainstein A, Weiss D. Rose
472   scent: genomics approach to discovering novel floral fragrance-related genes. Plant Cell
473   2002;14:2325-38.
474 Hauschild R, Schaewen AV. Differential regulation of glucose-6-phosphate dehydrogenase isoenzyme
475   activities in potato. Plant Physiol 2003;133:47-62.
476 Hayashi S, Yagi K, Ishikawa T, Kawasaki M, Asai T, Picone J, Turnbull C, Hiratake J, Sakata K,
477   Takada M, Ogawa K, Watanabe N. Emission of 2-phenylethanol from its β-D-glucopyranoside and
478   the biogenesis of these compounds from [^{2}H$_8$] L-phenylalanine in rose flowers. Tetrahedron
479   2004;60:7005-13.
480 Jollivet N, Bézenger MC, Vayssier Y, Belin JM. Production of volatile compounds in liquid cultures
481   by six strains of coryneform bacteria. Appl Microbiol Biotechnol 1992;36:790-94.
482 Jornvall H, Persson B, Krook M, Atrian S, Gonzalez-Duarte R, Jeffery J, Ghosh D. Short-chain
483   dehydrogenases/reductases (SDR). Biochemistry 1995;34:6003-13.
484 Kaminaga Y, Schnepp J, Peel G, Kish CM, Ben-Nissan G, Weiss D, Orlova I, Lavie O, Rhodes D,
485   Wood K, Porterfield DM, Cooper AJL, Schloss JV, Pichersky E, Vainstein A, Dudareva N. Plant
486   phenylacetaldehyde synthase is a bifunctional homotetrameric enzyme that catalyzes phenylalanine
487   decarboxylation and oxidation. J Biol Chem 2006;281:23357-66.
488 Larroy C, Fernandez MR, Gonzalez E, Pares X, Biosca JA. Characterization of the *Saccharomyces*
489   *cerevisiae YMR318C (ADH6)* gene product as a broad specificity NADPH-dependent alcohol
490   dehydrogenase: relevance in aldehyde reduction. Biochem J 2002;361:163-72.
491 Lavid N, Wang J, Shalit M, Guterman I, Bar E, Beuerle T, Menda N, Shafir S, Zamir D, Adam Z,
492   Vainstein A, Weiss D, Pichersky E, Lewinsohn E. *O*-Methyltransferases involved in the biosynthesis
493   of volatile phenolic derivatives in rose petals. Plant Physiol 2002;129:1899-907.
494 Mabberley DJ. Mabberley's Plant-Book. Cambridge: Cambridge University Press, 2008.
495 McCracken JA, Wang L, Kohen A. Synthesis of *R* and *S* tritiated reduced β-nicotinamide adenine
496   dinucleotide 2' phosphate. Anal Biochem 2004;324:131-6.
497 Mita S, Nagai Y, Asai T. Isolation of cDNA clones corresponding to genes differentially expressed in
498   pericarp of mume (*Prunus mume*) in response to ripening, ethylene and wounding signals. Physiol
499   Plant 2006;128:531-45.
500 Mostad SB, Glasfeld A. Using high field NMR to determine dehydrogenase stereospecificity with
501   respect to NADH. J Chem Educ 1993;70:504-6.
502 Niall HD. Automated Edman degradation: the protein sequenator. Methods Enzymol 1973;27:942-
503   1010.

504 Oka N, Ohishi H, Hatano T, Hornberger M, Sakata K, Watanabe N. Aroma evolution during flower
505   opening in *Rosa damascena* Mill. Z Naturforsch 1999;54c,889-95.
506 Okada T, Mikage M, Sekita S. Molecular characterization of the phenylalanine ammonia-lyase from
507   *Ephedra sinica*. Biol Pharm Bull 2008;31:2194-9.
508 Persson B, Jeffery J, Jörnvall H. Different segment similarities in long-chain dehydrogenases. Biochem
509   Biophys Res Commun1991;177:218-23.
510 Persson B, Zigler JJ, Jörnvall H. A super-family of medium-chain dehydrogenases/reductases (MDR).
511   Eur J Biochem 1994;226:15-22.
512 Persson B, Kallberg Y, Oppermann U, Jörnvall H. Coenzyme-based functional assignments of short-
513   chain dehydrogenases/reductases (SDRs). Chem Biol Interact 2003;143-144:271-8.
514 Pichersky E, Gershenzon J. The formation and function of plant volatiles: perfumes for pollinator
515   attraction and defense. Curr Opin Plant Biol 2002;5:237-43.
516 Rodopulo AK, Lyudnikova TA, Bezzubov AA. Effect of yeast cultivation conditions on the
517   biosynthesis and accumulation of aromatic substances. Appl Biochem Microbiol 1985;21:332-6.
518 Rusanov K, Kovacheva N, Vosman B, Zhang L, Rajapakse S, Atanassov A, Atanassov I. Microsatellite
519   analysis of *Rosa damascena* Mill. accessions reveals genetic similarity between genotypes used for
520   rose oil production and old Damask rose varieties. Theor Appl Genet 2005;111:804-9.
521 Sakai M, Hirata H, Sayama H, Sekiguchi K, Itano H, Asai T, Dohra H, Hara M, Watanabe N.
522   Production of 2-phenylethanol in roses as the dominant floral scent compounds from L-
523   phenylalanine by two key enzymes, a PLP-dependent decarboxylase and a phenylacetaldehyde
524   reductase. Biosci Biotechnol Biochem 2007;71:2408-19.
525 Serra S, Fuganti C, Brenna E. Biocatalytic preparation of natural flavours and fragrances. Trends
526   Biotechnol 2005;23:193-8.
527 Suzuiki M, Matsumoto S, Mizoguchi M, Hirata S, Takagi K, Hashimoto I, Yamano Y, Ito M,
528   Fleischmann P, Winterhalter P, Morita T, Watanabe N. Identification of (3*S*, 9*R*)- and (3*S*, 9*S*)-
529   megastigma-6,7-dien-3,5,9-triol 9-*O*-β-D-glucopyranosides as damascenone progenitors in the
530   flowers of *Rosa damascena* Mill. Biosci Biotechnol Biochem 2002;66:2692-7.
531 Tieman D, Taylor M, Schauer N, Fernie AR, Hanson AD, Klee HJ. Tomato aromatic amino acid
532   decarboxylases participate in synthesis of the flavor volatiles 2-phenyethanol and 2-
533   phenylacetaldehyde. Proc Natl Acad Sci 2006;103:8287-92.
534 Tieman DM, Loucas HM, Kim JY, Clark DG, Klee HJ. Tomato phenylacetaldehyde reductases
535   catalyze the last step in the synthesis of the aroma volatile 2-phenylethanol. Phytochemistry
536   2007;68:2660-9.
537 Watanabe S, Hayashi K, Yagi K, Asai T, MacTavish H, Picone J, Turnbull C, Watanabe N. Biogenesis
538   of 2-phenylethanol in rose flowers: incorporation of [^{2}H$_8$] L-phenylaninie into 2-phenylethanol
539   and its β-D-glucopyranoside during the flower opening of *Rosa* 'Hoh-jun' and *Rosa damascena*
540   Mill. Biosci Biotechnol Biochem 2002;66:943-7.
541 Zhang L, Kudo T, Takaya N, Shoun H. The B' helix determines cytochrome P450 nor specificity for
542   the electron donors NADH and NADPH. J Biol Chem 2002;277:33842-7.

543

544 **Tables**

545 **Table 1.** Peptide fragments of rose-PAR from *Rosa ×damascena*

546

MH$^+$	m/z	Charge	Sequence	Degenerate primer
839.4	420.2	2+	YCLVER	
908.5	454.8	2+	LWYVLSK	
955.5	478.2	2+	AELLDPAVK	
974.5	487.7	2+	YHDVTDPK	No. 1
1004.5	502.8	2+	TLAEDAAWK	No. 2
1076.6	538.8	2+	ETLESLKEK	
1167.7	584.3	2+	TEHLLALDGAK	
1192.6	596.8	2+	GTLNVLNSCSK	
1198.6	400.2	3+	ASVRNPNDPTK	

| 1512.8 | 756.9 | 2+ | TYPNASF | |
| 1868.9 | 623.6 | 3+ | DVANAHVQAFELPSASGR | No. 3 |

547

548

549 **Table 2.** Relative activities of the recombinant PAR and rose-PAR from *Rosa*

550 *×damascena* with selected substrates. Enzymatic activities with phenylacetaldehyde

551 were set as 100%. Data present the mean values ± standard error from triplicate

552 experiments.

Substrate	Recombinant PAR relative activity (%)	Rose- PAR relative activity (%)
Phenylacetaldehyde	100.0±4.9	100.0±1.4
(*S*)-(-)-Citronellal	311.2±8.7	78.4±2.3
Hexylaldehyde	186.0±6.5	66.4±1.7
(*R*)-(+)-Citronellal	96.9±4.9	46.6±1.2
3-Phenylpropionaldehyde	63.6±5.7	59.2±0.9
Benzaldehyde	47.3±4.4	54.0±2.8
trans-Cinnamaldehyde	40.3±4.2	14.8±0.9
2-Phenylpropionaldehyde	39.5±6.2	19.5±1.2
Citral	39.5±6.6	53.9±2.8
Acetophenone	28.7±3.9	7.0±1.0
Methyl butylketone	19.0±1.9	7.5±2.4

553

554 **Fig. 1.** Isolation and identification of rose-PAR by gel filtration chromatography and

555 SDS-PAGE. (A) PAR activity in gel filtration chromatographic fractions assayed by

556 absorbance changes of NADPH. (B) SDS-PAGE of chromatographic fractions 21-23.

557 The 35 kDa protein occurs in fraction 22 which had the highest enzymatic activity.

558 **Fig. 2.** Conversion from PAld to 2PE by the recombinant PAR expressed in *E. coli*

559 and rose-PAR. Products were separated by GC. The control assay was carried out
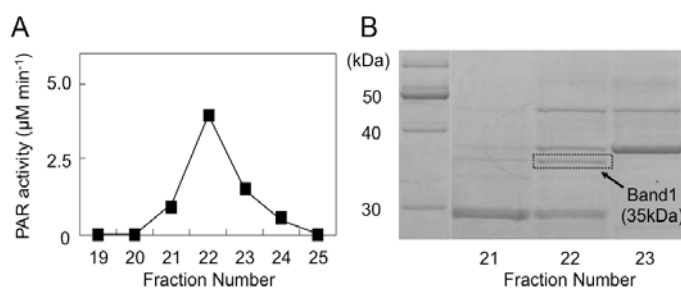
560 without enzyme.

561 **Fig. 3.** Relative transcripts expression levels of *PAR* in different rose tissues at

562 different stages. Values represented the ratio of *PAR* transcripts (from 50 ng RNA) to

563 *TUB*. Data shown represent the mean values ± standard deviation from triplicate

564 experiments.

565 **Fig. 4.** Coenzyme preference and direction of reactions catalyzed by PARs. A,

566 Coenzyme preference. PAR activity was assayed in the presence of 1mM NADPH or

567 NADH. The activity of the NADPH sample (1.5 mmol mg^{-1} protein h^{-1}) is regarded as

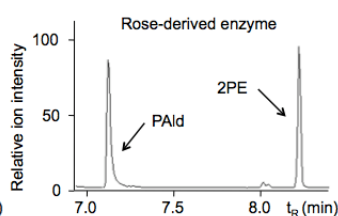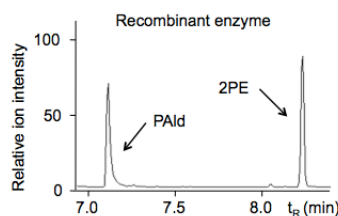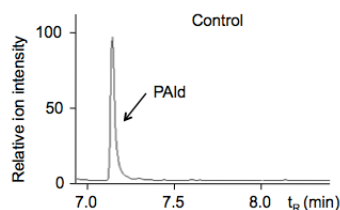568 100%. B, Reaction direction of PAR. Oxidative activity (ADH activity) for the

569   production of 2PE in the presence of NADP$^+$ was measured by GC-MS. The reaction

570   mixture contained 1mM 2PE, 1 mM NADP$^+$ and 30 µl of the main PAR fraction.

571   PAR activity (1.3 mmol mg^{-1} protein h^{-1}) was set as 100%. All data shown represent

572   the mean ± standard error from triplicate experiments.

573   **Fig. 5.** The selectivities of both recombinant and rose-derived PARs for the

574   conversion of PAld to 2PE in the presence of NADPH. Both NADPH enantiomers

575   were labeled with ^{2}H. The total amount of 2PE and [^{2}H]-2PE is set as 100%.

576   **Fig. 6.** GC analysis of the reaction products of acetophenone catalyzed by the

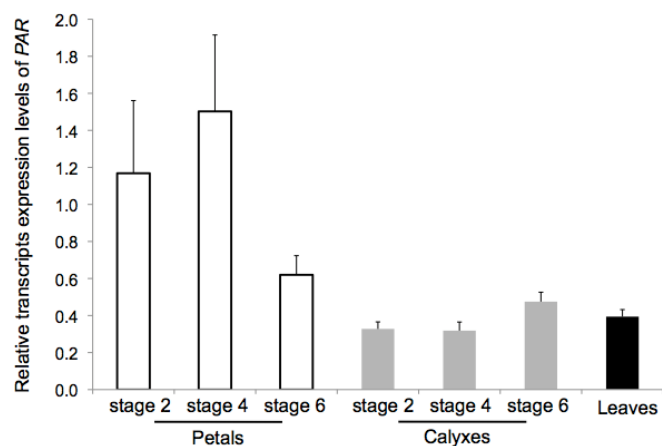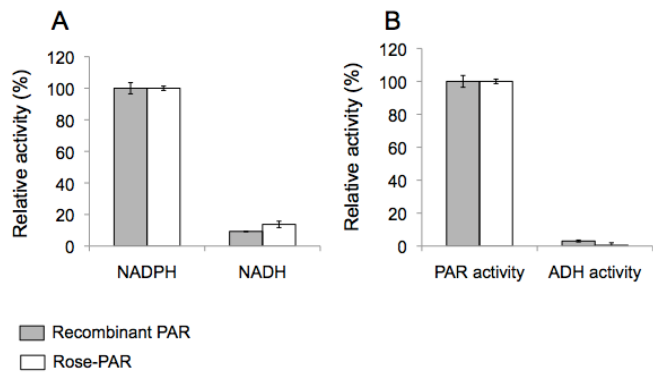577   recombinant PAR. A: total ion traces of authentic samples; B: reaction mixture.
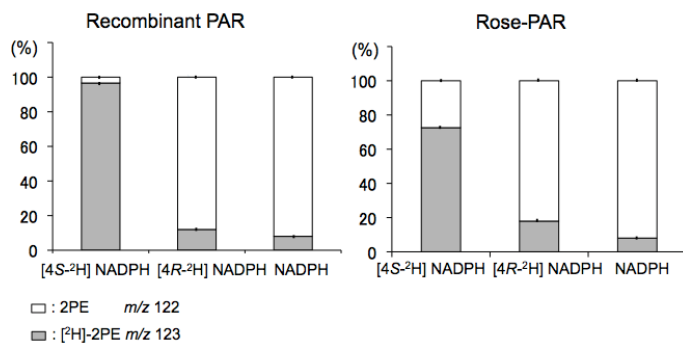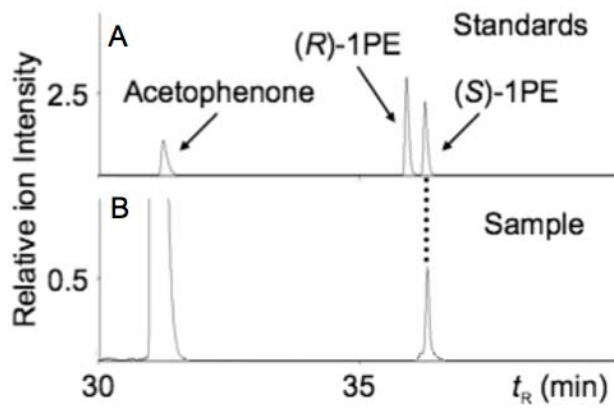
578

579

580

581

582

583

584

585